NOTE

Clinical Pathology

Intestinal gastrointestinal stromal tumor in a cat

Akihisa SUWA[1) and Tetsuya SHIMODA[1)*]

[1) Sanyo Animal Medical Center, 357-1 Komoto, Akaiwa, Okayama 709-0821, Japan

ABSTRACT. A 12-year-old, 3.6-kg, spayed female domestic shorthaired cat had a 2-month history of anorexia and weight loss. Abdominal ultrasonography and computed tomography revealed an exophytic mass originating from the jejunum with very poor central and poor peripheral contrast enhancement. On day 14, surgical resection of the jejunum and mass with 5-cm margins and an end-to-end anastomosis were performed. Histopathological examination revealed the mass was a transmural, invasive cancer showing exophytic growth and originating from the small intestinal muscle layer. Immunohistochemical analysis of tumor cells revealed diffuse positivity for KIT protein and negativity for desmin and S-100. The mass was diagnosed as a gastrointestinal stromal tumor (GIST). Ultrasonographic findings indicated the tumor probably metastasized to the liver and omentum, as seen in humans and dogs. The owner rejected further treatment at the last visit on day 192. To our knowledge, this is the first report of intestinal tumor and metastasis in feline GIST and its imaging features.

KEY WORDS: feline, gastrointestinal stromal tumor, intestinal tumor

Intestinal tumors are generally rare in cats. Lymphomas account for nearly 30% of all feline tumors and are the most common intestinal tumors [20]. Adenocarcinomas are the second most frequent tumors in cats, followed by mast cell tumors. Gastrointestinal stromal tumors (GISTs) are thought to originate from the interstitial cells of Cajal (ICCs), which form a network that coordinates peristalsis in the gastrointestinal tract [11]. Many of the smooth muscle tumors in human and canine patients have now been reclassified as GISTs, which by definition express CD117 (KIT) [13, 15]. GISTs have been described in humans, dogs, horses, Spanish ibex, a ferret, a rat, and nonhuman primates [5, 18, 19]. These occur most frequently in the jejunum, cecum and colon [16]. To the authors' knowledge, only one report has described "a feline GIST" in the stomach [17].

A 12-year-old, 3.6-kg, spayed female domestic shorthaired cat with a body condition score of 2/5 presented with a 2-month history of anorexia and weight loss. On physical examination, the animal had a palpable large mass (about 5.0 cm) in the abdomen. No lymphadenopathies were noted at the superficial lymph nodes. A complete blood count test revealed a low packed cell volume (PCV, 24.0%; reference range, 30.3–52.3%), neutrophilia (21,141/μl; reference range, 2,500–12,500/μl) and monocytosis (1,292/μl; reference range, 0–850/μl). A serum biochemical profile revealed hypoalbuminemia (2.6 g/dl; reference range, 2.7–3.8 g/dl) and hyperglobulinemia (5.4 g/dl; reference range, 2.8–5.1 g/dl). The serum protein fraction was normal. Enzyme-linked immunosorbent assays for feline leukemia virus and feline immunodeficiency virus yielded negative results. Radiography indicated a large mass in the abdomen. Abdominal ultrasonography revealed a hypoechoic mass (approximately 41.8 × 60.6 mm) containing hyperechoic and hypoechoic areas of unknown origin and a nodule (approximately 8.4 × 9.5 mm) containing a hypoechoic rim and an isoechoic center in the left lateral lobe of the liver (Fig. 1A and 1B). Moreover, ultrasound-guided fine-needle aspiration of the large mass showed mostly macrophages and neutrophils. Polymerase chain reaction analysis of the abdominal mass sample was negative for feline coronavirus. On day 7, contrast-enhanced computed tomography (CT) was performed under anesthesia. Iopamidol (300 mg I/ml, Oypalomin injection 300; Fuji Pharma Co., Ltd., Toyama, Japan) was used as the contrast medium at a dose of 2 ml/kg and was injected using a power injector over 15 to 20 sec via the jugular vein. Images were acquired before contrast medium injection, in an arterial phase (20 sec), in a portal phase (40 sec) and at equilibrium (180 sec) after contrast medium injection. CT examination revealed the exophytic mass originating from the jejunum. It had very poor contrast enhancement centrally and poor contrast enhancement peripherally (Fig. 1C). It was assumed to reflect a cavity of necrotic tissue. In the left lateral lobe of the liver, the hypoattenuating nodule was observed in all the phases (Fig. 1D). We concluded that the mass originated from the jejunum and could be surgically resected. On day 14, laparotomy was used to expose the mass originating from the jejunum that had an irregular surface and adhesive omentum. Surgical resection of the jejunum including the mass with 5-cm margins and an end-to-end anastomosis were performed (Fig. 2A). During surgery, we found enlargement of mesenteric lymph nodes

*Correspondence to: Shimoda, T., Sanyo Animal Medical Center, 357-1 Komoto, Akaiwa, Okayama 709-0821, Japan. e-mail: shimoda@sanyo-amc.jp
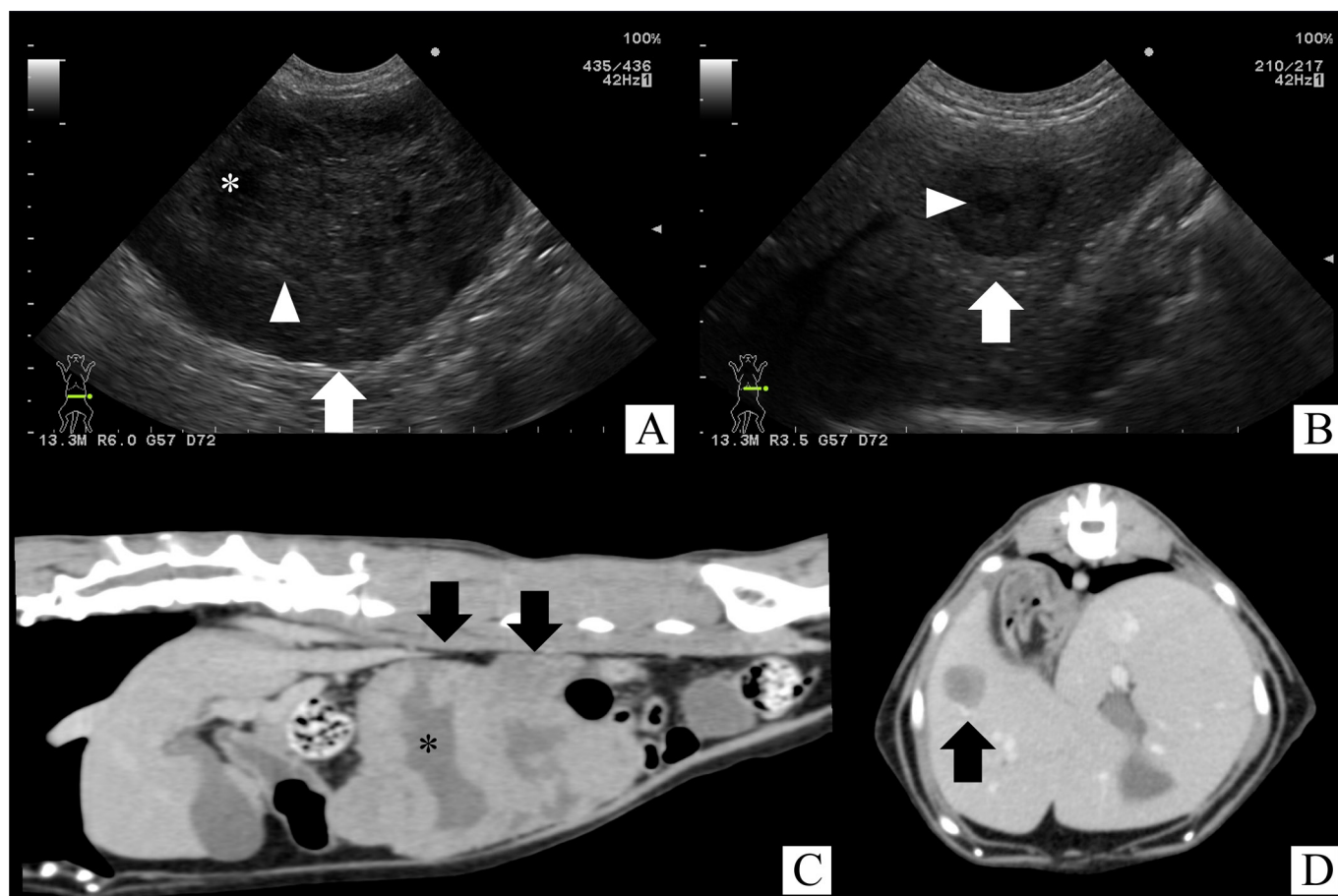
Fig. 1. Preoperative ultrasonography and computed tomography (CT) images: (A) a large hypoechoic mass (approximately 41.8 × 60.6 mm) (arrow) containing hyperechoic (arrowhead) and hypoechoic (asterisk) areas of unknown origin and (B) a hepatic nodule (approximately 8.4 × 9.5 mm) (arrow) containing a hypoechoic rim and isoechoic center (arrowhead) on ultrasonography performed on day 1. (C) Sagittal image indicates a large extramural mass (arrow) arising from the small intestine and containing regions of cavitation (asterisk). (D) A transverse image of the liver indicates a nodule with lower attenuation (arrow) than that of the normal surrounding parenchyma on CT performed on day 7.

(approximately 5.0 mm) (Fig. 2B) and performed cytological examination of a fine-needle aspirate. It revealed the lymph node had reactive hyperplasia. Biopsy examination of a hepatic nodule was not performed, because the owner declined it. After surgery, the cat was administered total parenteral nutrition through a central venous catheter.

Histopathological examination of the mass revealed that it was a poorly demarcated and invasive lesion that grew by forming an exophytic nodule from the muscular layer to the serosal surface of the intestine. The nodule comprised tumor cells arranged as interlacing fascicles in a storiform pattern, with homogenously oval nuclei and spindle-shaped cytoplasm or pleomorphism with indistinct boundaries (Fig. 2C). Mitotic figures were uncommon and ranged from 0 to 1 per 10 high-power fields. A clump of cancer cells was found in the lymphatic vessels, and some tumor cells were observed on the one-sided muscular layer margins. Multifocal and wide areas of hemorrhage and necrosis were also observed. Differential diagnoses included gastrointestinal mesenchymal tumors, notably GIST, leiomyosarcoma and peripheral nerve sheath tumor. Immunohistochemical analysis showed that the tumor cells were diffusely positive for KIT protein (polyclonal rabbit anti-human CD117; Dako, Carpinteria, CA, U.S.A.) (Fig. 2D), and negative for desmin (mouse monoclonal anti-human Desmin; Bio Genex, Fremont, CA, U.S.A.) and S-100 protein (rabbit polyclonal anti-S100; Dako). On the basis of the above results, the mass was finally diagnosed as an intestinal GIST.

On postoperative day 15, the cat was transfused whole blood (about 35.0 ml) and administered low-molecular-weight heparin (Dalteparin Na; Nichiiko Co., Ltd., Toyama, Japan), 100 U/kg body weight intravenously at constant-rate infusion until discharge, because of decreasing PCV (11.0%) and platelet count (125×10^3/μl; reference range, 151–600×10^3/μl). On day 18, the cat was transfused whole blood (about 30.0 ml) again, because of decreasing PCV (16.0%). The cat was discharged from a hospital on day 20 and was followed up with no therapy, because of difficulty to being administered drugs by owner. On day 77, the cat was improved anorexia and anemia. Abdominal ultrasonography revealed enlargement of the nodule in the left lateral lobe (approximately 14.0 mm) and a new hypoechoic lesion in the caudal left renal region (approximately 7.0 mm) (Fig. 3A). Ultrasound-guided fine-needle aspiration of the new region showed spindle-shaped cells with some nucleoli (Fig. 3B). On day 155, the cat showed clinical signs including anorexia, ascites and anemia (PCV, 13.0%). The nodule in the left lateral lobe enlarged
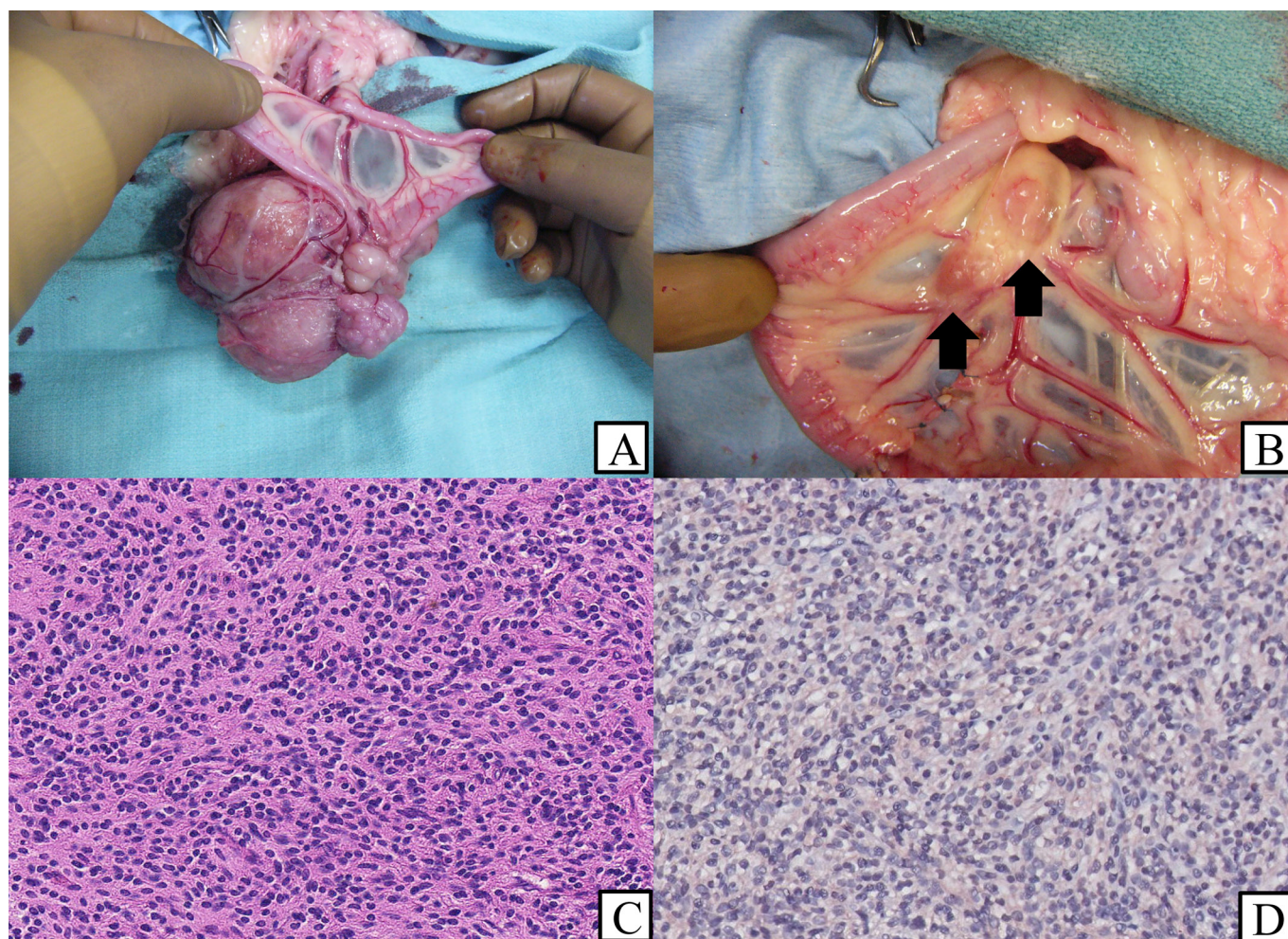
Fig. 2. (A) Laparotomy reveals a mass originating from the jejunum that has an irregular surface and adhesive omentum, and (B) enlargement of the mesenteric lymph nodes (approximately 5.0 mm) (arrows) on day 14. Histopathological examination of the mass. (C) Transmural, invasive cancer showing exophytic growth originating from the muscle layer of the small intestine. The tumor comprises spindle-shaped cells arranged as interlacing fascicles or in a storiform pattern with indistinct boundaries (hematoxylin and eosin staining at ×20). (D) Tumor cells are diffusely positive for KIT protein (CD117) (immunohistochemical staining at ×20).

(approximately 22.8 mm), and the hypoechoic lesions in the caudal left renal region expanded and indicated metastasis to the omentum (Fig. 3D). The owner rejected further treatment at the last visit on day 192.

GISTs are most common in the stomach (60–70%), followed by the small intestine (20–25%), colon and rectum (5%), and esophagus (<5%) in humans [14]. In dogs, GISTs occur most commonly in the large intestine, including the cecum, colon and rectum (48–67%), followed by the small intestine (29–30%) and stomach (0–19%) [5, 7, 18]. Only one previous report has documented the occurrence of a GIST in the stomach of a cat [17]. In the present case, the GIST occurred in the small intestine. These findings indicate that feline GISTs could occur anywhere in the gastrointestinal tract, as seen in humans and dogs.

GISTs have recently been recognized and defined as CD117-positive spindle or epithelioid neoplasms [14]. In this case, the tumor cells were diffusely positive for KIT protein and negative for desmin and S-100 protein as seen in the previous report [16, 17]. This report may confirm that CD117 is a useful diagnostic marker for feline GISTs. Mutations of the *c-kit* gene have been identified in exons 9 (5–10%) and 11 (60–70%) in cases of human GIST [3] and in exon 11 in cases of canine and feline GISTs [5, 6]. There was an overlap between canine and feline GIST mutations with one of the hotspots of driver mutations in human GISTs [12]. Unfortunately, the *c-kit* gene mutation could not be analyzed in this case, because of poor preservation of samples. Determining whether a tumor is KIT positive is essential in human and canine patients, and even in cats, because of the possibility of medical treatment with imatinib mesylate when the tumor is nonresectable, or in case of recurrence after surgery or metastases [10, 11].

In this case, the propensity of GIST to metastasize to the abdominal cavity and liver, as is typical in human and canine GISTs [2, 5, 7], was also documented. On CT, the mass had a heterogeneously enhancing soft-tissue rim surrounding a necrotic center, and the hepatic lesion appeared as a hypoattenuating nodule in all the phases. On ultrasonography, the mass and the hepatic and omentum lesions also had heterogeneous patterns with internal areas of lower echogenicity. In the hepatic lesion, we identified
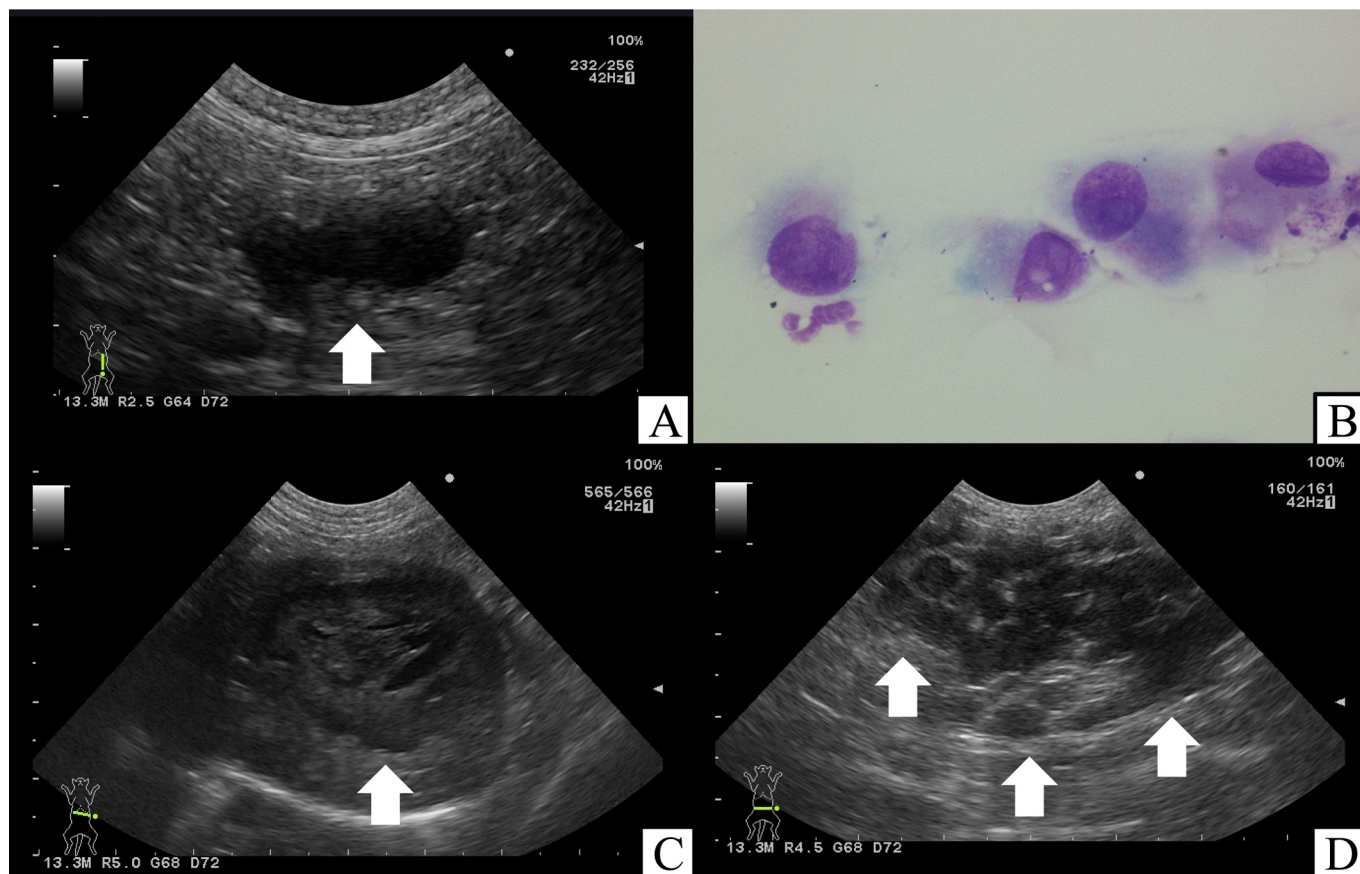
Fig. 3. (A) Abdominal ultrasonography reveals a new hypoechoic lesion (arrow) at the caudal left renal region, and (B) ultrasound-guided fine-needle aspiration of the region shows spindle-shaped cells with some nucleoli (Wright-Giemsa staining at ×400) on day 77. (C) On day 155, enlargement of the nodule (arrow) in the left lateral lobe and (D) expansion of the hypoechoic lesions (arrows) at the caudal left renal region are seen.

a hypoechoic rim and an isoechoic center, called a "cavitary target lesion." In dogs and cats, target lesions have been associated principally with malignant hepatic tumors, hepatic metastasis and hepatic lymphoma [4]. In humans, ultrasonographic features of GISTs include a large extramural tumor arising from the muscularis layer, which rarely affects the mucosal layer and often contains regions of cavitation. Additionally, the features suggesting high malignant potential were size and internal heterogenicity with the presence of intratumoral hypoechoic areas [21]. Furthermore, Burkill *et al.* described that on CT, the metastases within the liver were all of lower attenuation than that seen in the normal surrounding parenchyma in patients with GIST [2]. In dogs, some reports have described the ultrasonographic features of GISTs. Despite the overlap of the appearances of GISTs and other sarcomatous tumors, these imaging features might highly suggest the presence of a GIST [8, 9]. Therefore, in this case, the hepatic and omentum lesions might indicate the metastases of GIST. No previous reports have documented these imaging features or the occurrence of metastasis in feline GIST, but our findings indicate that feline GISTs have a similar biologic behavior to human and canine GISTs.

A recent study showed that tumor diameter was an important prognostic factor and mitotic count was a less significant factor in cases of canine GISTs [16]. In humans, two prognostic factors, tumor size and mitotic index, are known to provide the most useful histologic indication of the future biologic behavior of the tumor [1]. These factors indicate that large tumors (larger than 5 cm) with a high mitotic count (more than 50 mitotic figures per 50 high-power fields) commonly metastasize. In this case, the cat had a large tumor size and a low mitotic count, but the GIST metastasized after surgery. However, no definitive prognostic criteria for tumor size and mitotic count are yet available for animal GISTs.

To our knowledge, this is the first report of the occurrence of intestinal tumor and metastasis in feline GIST, and to describe the imaging features similar to those described in dogs and humans. Few reports have described feline GIST, and its biologic behaviors, treatments, and imaging and pathologic features remain unclear. Studies with greater numbers of cases are warranted, and the current case findings will contribute to future studies on feline GIST.

REFERENCES

1. Berman, J. and O'Leary, T. J. 2001. Gastrointestinal stromal tumor workshop. *Hum. Pathol.* **32**: 578–582. [Medline] [CrossRef]
2. Burkill, G. J., Badran, M., Al-Muderis, O., Meirion Thomas, J., Judson, I. R., Fisher, C. and Moskovic, E. C. 2003. Malignant gastrointestinal stromal tumor: distribution, imaging features, and pattern of metastatic spread. *Radiology* **226**: 527–532. [Medline] [CrossRef]
3. Corless, C. L., Barnett, C. M. and Heinrich, M. C. 2011. Gastrointestinal stromal tumours: origin and molecular oncology. *Nat. Rev. Cancer* **11**: 865–878. [Medline]
4. Cuccovillo, A. and Lamb, C. R. 2002. Cellular features of sonographic target lesions of the liver and spleen in 21 dogs and a cat. *Vet. Radiol. Ultrasound* **43**: 275–278. [Medline] [CrossRef]
5. Frost, D., Lasota, J. and Miettinen, M. 2003. Gastrointestinal stromal tumors and leiomyomas in the dog: a histopathologic, immunohistochemical, and molecular genetic study of 50 cases. *Vet. Pathol.* **40**: 42–54. [Medline] [CrossRef]
6. Gregory-Bryson, E., Bartlett, E., Kiupel, M., Hayes, S. and Yuzbasiyan-Gurkan, V. 2010. Canine and human gastrointestinal stromal tumors display similar mutations in c-KIT exon 11. *BMC Cancer* **10**: 559. [Medline] [CrossRef]
7. Gillespie, V., Baer, K., Farrelly, J., Craft, D. and Luong, R. 2011. Canine gastrointestinal stromal tumors: immunohistochemical expression of CD34 and examination of prognostic indicators including proliferation markers Ki67 and AgNOR. *Vet. Pathol.* **48**: 283–291. [Medline] [CrossRef]
8. Hanazono, K., Fukumoto, S., Hirayama, K., Takashima, K., Yamane, Y., Natsuhori, M., Kadosawa, T. and Uchide, T. 2012. Predicting metastatic potential of gastrointestinal stromal tumors in dog by ultrasonography. *J. Vet. Med. Sci.* **74**: 1477–1482. [Medline] [CrossRef]
9. Hobbs, J., Sutherland-Smith, J., Penninck, D., Jennings, S., Barber, L. and Barton, B. 2015. Ultrasonographic features of canine gastrointestinal stromal tumors compared to other gastrointestinal spindle cell tumors. *Vet. Radiol. Ultrasound* **56**: 432–438. [Medline] [CrossRef]
10. Kobayashi, M., Kuroki, S., Ito, K., Yasuda, A., Sawada, H., Ono, K., Washizu, T. and Bonkobara, M. 2013. Imatinib-associated tumour response in a dog with a non-resectable gastrointestinal stromal tumour harbouring a c-kit exon 11 deletion mutation. *Vet. J.* **198**: 271–274. [Medline] [CrossRef]
11. Koh, J. S., Trent, J., Chen, L., El-Naggar, A., Hunt, K., Pollock, R. and Zhang, W. 2004. Gastrointestinal stromal tumors: overview of pathologic features, molecular biology, and therapy with imatinib mesylate. *Histol. Histopathol.* **19**: 565–574. [Medline]
12. Lasota, J., Jasinski, M., Sarlomo-Rikala, M. and Miettinen, M. 1999. Mutations in exon 11 of c-Kit occur preferentially in malignant versus benign gastrointestinal stromal tumors and do not occur in leiomyomas or leiomyosarcomas. *Am. J. Pathol.* **154**: 53–60. [Medline] [CrossRef]
13. Maas, C. P. H. J., ter Haar, G., van der Gaag, I. and Kirpensteijn, J. 2007. Reclassification of small intestinal and cecal smooth muscle tumors in 72 dogs: clinical, histologic, and immunohistochemical evaluation. *Vet. Surg.* **36**: 302–313. [Medline] [CrossRef]
14. Miettinen, M. and Lasota, J. 2001. Gastrointestinal stromal tumors--definition, clinical, histological, immunohistochemical, and molecular genetic features and differential diagnosis. *Virchows Arch.* **438**: 1–12. [Medline] [CrossRef]
15. Miettinen, M., El-Rifai, W., H L Sobin, L. and Lasota, J. 2002. Evaluation of malignancy and prognosis of gastrointestinal stromal tumors: a review. *Hum. Pathol.* **33**: 478–483. [Medline] [CrossRef]
16. Morini, M., Bettini, G., Preziosi, R. and Mandrioli, L. 2004. C-kit gene product (CD117) immunoreactivity in canine and feline paraffin sections. *J. Histochem. Cytochem.* **52**: 705–708. [Medline] [CrossRef]
17. Morini, M., Gentilini, F., Pietra, M., Spadari, A., Turba, M. E., Mandrioli, L. and Bettini, G. 2011. Cytological, immunohistochemical and mutational analysis of a gastric gastrointestinal stromal tumour in a cat. *J. Comp. Pathol.* **145**: 152–157. [Medline] [CrossRef]
18. Russell, K. N., Mehler, S. J., Skorupski, K. A., Baez, J. L., Shofer, F. S. and Goldschmidt, M. H. 2007. Clinical and immunohistochemical differentiation of gastrointestinal stromal tumors from leiomyosarcomas in dogs: 42 cases (1990−2003). *J. Am. Vet. Med. Assoc.* **230**: 1329–1333. [Medline] [CrossRef]
19. Saturday, G. A., Lasota, J., Frost, D., Brasky, K. B., Hubbard, G. and Miettinen, M. 2005. KIT-positive gastrointestinal stromal tumor in a 22-year-old male chimpanzee (Pan troglodites). *Vet. Pathol.* **42**: 362–365. [Medline] [CrossRef]
20. Selting, K. A. 2012. Intestinal Tumors. pp. 412–423. *In*: Small Animal Clinical Oncology. 5th ed. (Withrow, S.J. and Mac-Ewen, E.F. eds.), WB Saunders Co., Philadelphia.
21. Wronski, M., Cebulski, W., Slodkowski, M. and Krasnodebski, I. W. 2009. Gastrointestinal stromal tumors: ultrasonographic spectrum of the disease. *J. Ultrasound Med.* **28**: 941–948. [Medline] [CrossRef]